Clays and Clay Minerals, Vol. 22, pp. 175–183. Pergamon Press 1974. Printed in Great Britain

GAS SORPTION IN CLAY MINERAL SYSTEMS

L. A. G. AYLMORE

Department of Soil Science and Plant Nutrition, Institute of Agriculture,
University of Western Australia, Nedlands, W.A. 6009, Australia

(*Received* 14 *June* 1973)

Abstract—Sorption isotherms for four gases (N_2, A, Kr and CO_2), commonly used in specific surface area and pore structure measurements, have been accurately determined on a number of clay mineral and oxide systems.

Specific surface areas obtained by application of the BET theory to these isotherms illustrate the extent to which the apparent cross-sectional areas for these sorbed gases vary with surface structure, exchangeable cation and microporosity.

V–n plots for nitrogen adsorption on these materials using nitrogen adsorption on crystalline materials of large crystal size as a standard isotherm provide appreciable ranges of linearity in each case. The specific surface areas obtained from these straight line plots agree well with the corresponding BET values. The linearity of these plots for illite clays indicates the absence of capillary condensation and that adsorption in slit-shaped pores takes place largely by the formation of physically adsorbed layers on the surfaces.

Much larger BET specific surface areas were obtained from carbon dioxide sorption at 196 K on goethite, hematite and gibbsite than from nitrogen, argon and krypton sorption at 78°K. It is suggested that enhanced sorption of CO_2 into microporous regions of the oxides, inaccessible to the other gases, occurs in a similar fashion to that frequently observed for coal and charcoal materials. V–n plots for CO_2 sorption in these materials using that for an illite clay as a standard isotherm, support this conclusion.

Considerably lower BET specific surface areas were obtained for CO_2 sorption on kaolinite than were obtained for nitrogen, argon and krypton sorption. The shape of the V–n plots for CO_2 sorption on kaolinite compared with illite suggest that an initial specific adsorption of CO_2 on the kaolinite is followed by a change in state with the completion of this layer, allowing normal multilayer formation to proceed.

INTRODUCTION

The specific surface area and pore structure of a compacted clay system are undoubtedly two of its most important characteristics in determining both its chemical and physical interactions with its surroundings. Most chemical reactions in soils take place at the surface of the pores, and experimental studies of such reactions are almost invariably referred back to a unit area basis. Similarly the interpretation of physical properties such as swelling behavior, aggregate structure formation, and permeability requires an accurate measurement of specific surface area and a knowledge of the pore structure.

The most universally accepted method of determining the surface area of finely divided and porous materials is that of Brunauer, Emmett and Teller (1938), the BET method. A number of gases have been utilized in the application of this method to the physical adsorption of gases at low temperature. Since the method is accepted, sometimes without question, by numerous workers concerned with the properties of clays and clay minerals, it is important to establish the limits within which such acceptance can be sustained for the different gases in use.

When vapor adsorption methods were first developed, Emmett and Brunauer (1937) advocated the use of nitrogen as adsorbate, and this gas has been generally accepted as the most satisfactory. However, use of nitrogen as the primary standard has recently been questioned (Aristov and Kiselev, 1963; Pierce and Ewing, 1964), there being suggestions that the quadrupole moment of nitrogen can interact with hydroxyl or other polar groups, leading to a change in the cross-sectional area of the adsorbed molecule.

Argon adsorption at 78°K has been preferred by some workers, since this is a symmetrical non-polar atom which should be less subject to specific interactions affected by changes in the chemical nature of surfaces. However argon is less strongly adsorbed than nitrogen, raising some doubts as to whether the BET procedure provides a satisfactory estimate of the monolayer capacity ($C < 50$). Also there are strong suggestions that the effective saturation vapor pressure (p_0) for argon varies between that for solid argon above non-porous materials to that of the supercooled liquid within micro- (< 20 Å) and transitional (20—200 Å) pores (Harris and Sing, 1967; Carruthers *et al.*, 1971).

Carbon dioxide adsorption at 196°K has been favored and extensively used in studies on carbon blacks, charcoals and similar materials (Anderson, Bayer and Hofer, 1965; Walker and Kini, 1965). The surface areas obtained using carbon dioxide on these materials frequently vastly exceed those obtained by nitrogen adsorption at 78°K, indicating the presence of large volumes of microporous regions inaccessible to the less energetic nitrogen adsorption. Similar effects have been noted with the expanding lattice alumino–silicates such as montmorillonite and vermiculite (Thomas and Bohor, 1968; Aylmore, Sills and Quirk, 1970).

For the measurement of very small surface areas ($<1\ m^2\ g^{-1}$) krypton sorption at 78°K has the advantage of providing a low saturation vapor pressure at the working temp. and hence a marked reduction in the volume of unadsorbed gas which has to be corrected for (Beebe, Beckwith and Honig, 1945; Sing and Swallow, 1960). Krypton adsorption also offers the benefit that its inertness makes it unlikely that it will interact specifically with the solid surface.

Because krypton and carbon dioxide sorption at 78 and 196°K respectively, like that of argon at 78°K, take place below the bulk triple point, the use of these two gases in specific surface area measurements is likewise subject to considerable uncertainty in the correct values for saturation vapour pressure to be used in the BET analysis.

Uncertainties in the validity of the BET approach when micro- and transitional pores are present (Gregg and Sing, 1967) and in the absolute values of molecular areas and how these will vary with substrate, have led to the recent development of alternative methods for comparison of adsorption isotherms. Amongst these the *t*-method of Lippens and De Boer (1965) and similar variations (Sing, 1968; Pierce, 1968) have attracted attention as a means of interpreting vapor adsorption isotherms and characterizing the porosity of solid adsorbents. These methods involve the use of 'reduced isotherms' in which the volume adsorbed V, is plotted against the corresponding statistical thickness (t) of the adsorbed layer on a non-porous reference solid (Lippens and de Boer, 1965), or alternatively against some arbitrarily chosen parameter $V_s = V/V_x$, where V_x is the volume adsorbed at $p/p_0 = 0{\cdot}4$ (Sing, 1968). Where adsorption results entirely from monolayer–multilayer formation straight line plots with slope proportional to the surface area of the sample will be obtained. The presence of complications such as specificity in adsorption, micropore filling and capillary condensation will almost invariably result in characteristic deviations from linearity (Gregg and Sing, 1967). Pierce (1968) has pointed out the advantage of V–n plots where n is the number of statistical layers on a reference standard, since these give directly the value of V_m, while t values are themselves based on n values and involve an assumption about the thickness of an adsorbed layer.

Considerable use has been made of V–n plots to examine nitrogen sorption in a variety of materials. In the present work this approach has been used to illustrate features of both nitrogen and CO_2 sorption in clay mineral and sesquioxide systems.

MATERIALS AND METHODS

The clay samples used were obtained from the following natural deposits:

Fithian illite—From Ward's Natural Science Establishment Inc., Illite No. 35 of the American Petroleum Institute Research Project No. 49 (1951).

Willalooka illite—B horizon from a solonized solonetz: Hundred of Laffer, South Australia.

A.P.I. No. 5 kaolinite—From Ward's Natural Science Establishment Inc., Kaolinite No. 5 of the American Petroleum Institute Research Project No. 49 (1951).

In general, samples of the clays were sodium saturated by repeated washing and centrifuging with molar sodium chloride during which the pH of the suspension was adjusted to 3·0 using HCl. The samples were washed and dialysed against distilled water using Visking cellulose casing, and the $<2\ \mu m$ fractions obtained by accurate sedimentation.

Samples saturated with cesium, calcium and lanthanum were prepared from the Na saturated suspensions by repeated washing with the appropriate molar chloride solution and finally with distilled water using dialysis tubing. During this procedure extreme care was taken to ensure that no material was lost from the samples.

The air-dried clays were gently ground to a powder, equilibrated with 0·75 relative water vapor pressure and compressed into 200 mg cores to facilitate subsequent handling. Previous studies have shown that this compaction into cores has little if any effect on the specific surface area or micropore structure of the clays.

Gibbsite was prepared by adding 4 N sodium hydroxide to 1 M hydrated aluminum chloride until the pH remained constant at 4·6. The precipitate formed was heated for 2 hr at 40°C and then dialysed in cellulose bags against distilled water for 28 days.

Goethite was prepared by dissolving 400 g ferric nitrate in 1800 ml water and adding approx 1500 ml of 2·5 M sodium hydroxide solution at 60°C over a period of some 24 hr to raise the pH to 12.

To prepare hematite 100 g of ferric nitrate was placed in 400 ml of water and refluxed for 3 weeks.

The materials were air dried and lightly compressed into 200 mg cores. In each case the preparations were verified by X-ray diffraction analysis.

Sorption isotherms were determined using standard volumetric equipment based on that described by Emmett and Brunauer (1934) and including many of the refinements suggested by Harkins and Jura (1944) and Joyner (1949). In general the aluminosilicate clay minerals and hematite samples were outgassed overnight at 300°C and 10^{-6} mm mercury pressure. The goethite and gibbsite samples were outgassed at 60°C to avoid decomposition of the samples. Provided the pressure in the system remained below 10^{-3} mm mercury pressure after 20 min isolation from the pumps the sample was regarded as thoroughly outgassed.

Nitrogen, argon and krypton adsorption isotherms were determined by the usual doser technique after immersing the sample bulb in a liquid nitrogen bath. Carbon dioxide adsorption isotherms at 195°K were obtained by immersing the sample bulb in a gently stirred solid carbon dioxide–ethanol slush. In between individual isotherms the samples were outgassed overnight at room temp. Nitrogen, argon and carbon dioxide pressures were measured using a wide bore manometer and cathetometer; krypton pressures by means of a McLeod gauge. Nitrogen, argon and carbon dioxide adsorption isotherms were measured to the appropriate saturation pressures while only sufficient adsorption points to provide accurate specific surface area calculations were obtained for krypton.

RESULTS AND DISCUSSION

Isotherms

The isotherms obtained for nitrogen, argon and carbon dioxide adsorption on the various materials are shown in Figs. 1–4. For nitrogen and argon the saturation vapor pressures, measured on an appropriate vapor pressure thermometer with the bulb immersed in the bath alongside the sample bulb, have been used to calculate the relative pressure (p/p_0). For carbon dioxide and krypton the extrapolated vapor pressures for the super-cooled liquids at the temperature of the bath have been used in calculating p/p_0. The validity of this latter procedure has been discussed by various authors (Beebe *et al.*, 1945; Gregg and Sing, 1967, pp. 84 and 90). It is used here since more linear plots were obtained in applying the BET theory than when the measured saturation vapor pressure was used.

The values for specific surface areas obtained by application of the BET theory to the various adsorption isotherms using the molecular areas and saturation

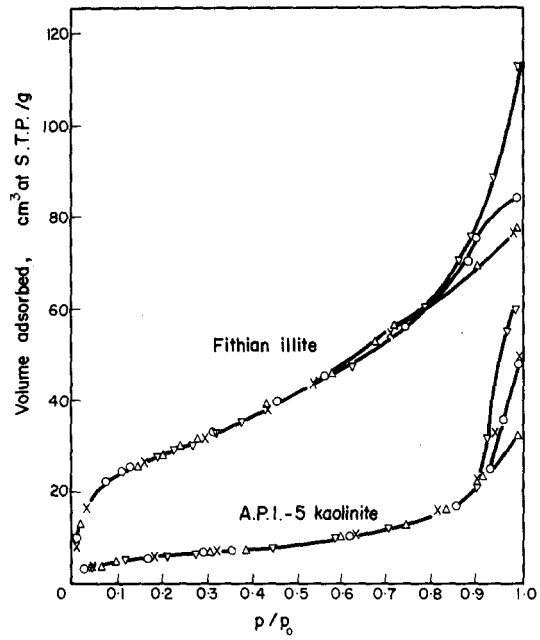

Fig. 1. Argon adsorption isotherms on homoionic Fithian illite and A.P.I.–5 kaolinite; × sodium, ○ caesium, △ calcium, ▽ lanthanum.

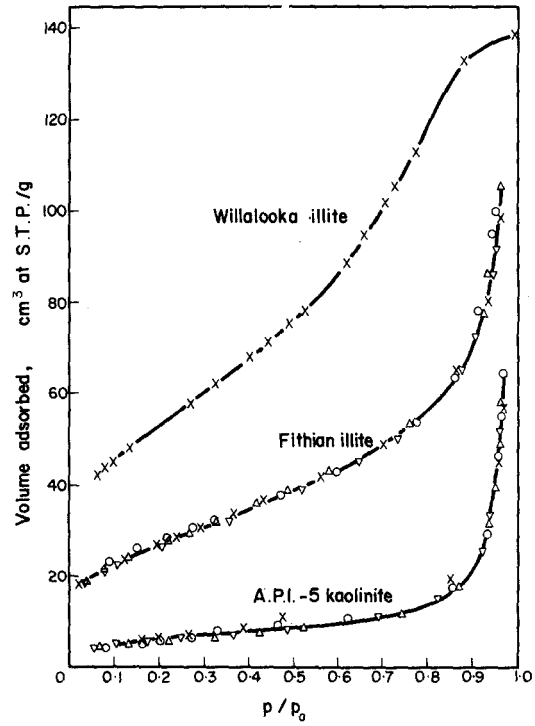

Fig. 2. Nitrogen adsorption isotherms on homoionic Willalooka illite, Fithian illite and A.P.I.–5 kaolinite; × sodium, ○ caesium, △ calcium, ▽ lanthanum.

https://doi.org/10.1346/CCMN.1974.0220205 Published online by Cambridge University Press

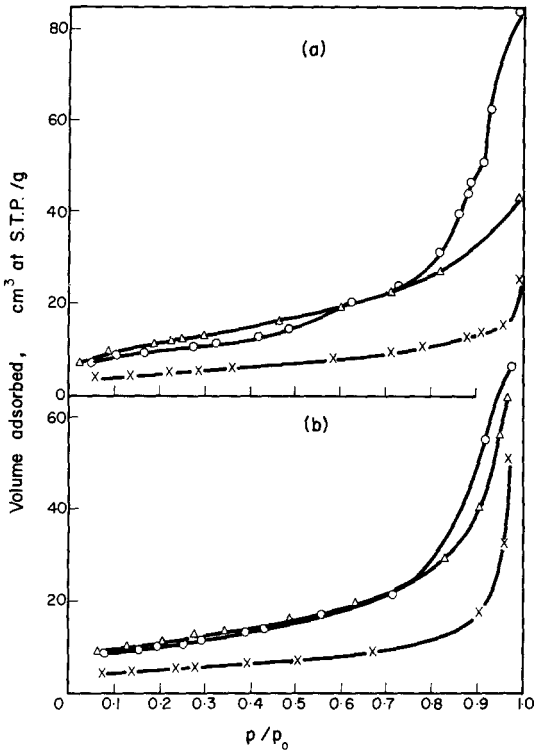

Fig. 3. (a) Argon adsorption isotherms and (b) Nitrogen adsorption isotherms on △ goethite, × hematite and ○ Gibbsite.

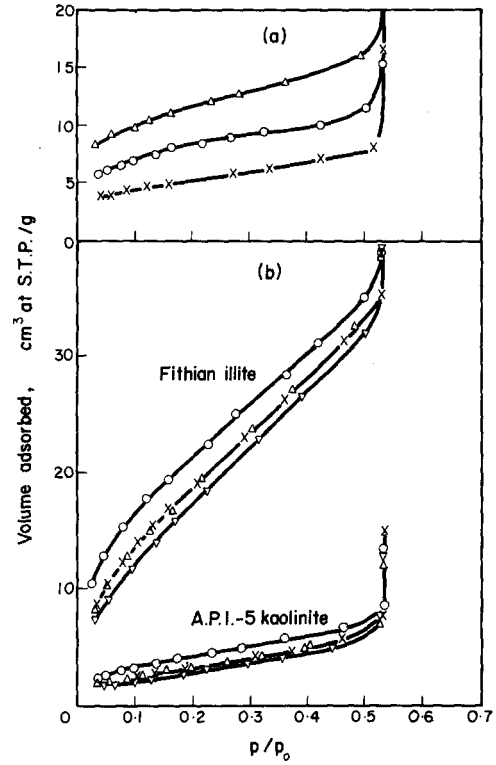

Fig. 4. Carbon dioxide adsorption isotherms on (a) △ goethite, × hematite and ○ gibbsite (b) homoionic fithian illite and A.P.I.-5 kaolinite; × sodium, ○ caesium, △ calcium, ▽ lanthanum.

vapor pressures indicated are given in columns 2–5 of Table 1.

Careful examination of the isotherms reveals a number of interesting features. At lower relative vapor pressures (p/p_0 < approx. 0·6) the argon isotherms for the Fithian illite and A.P.I.–5 kaolinite (Fig. 1) exhibit excellent reproducibility between the various ion exchanged forms of each clay. This reproducibility is reflected in the excellent agreement in specific surface areas obtained by application of the BET theory to these isotherms (column 3, Table 1). However, at high relative vapor pressures there are marked divergences between the isotherms obtained on the different cation-exchanged forms of each clay. The nitrogen isotherms for the different samples of each clay (Fig. 2) show slightly less reproducibility at low relative vapor pressures (cf. BET areas, Table 1) than was obtained using argon, but within these limits essentially the same isotherm is obtained for the various samples of each clay over the full range of relative vapor pressure to saturation.

The divergence of the argon isotherms at relative vapor pressures above the onset of capillary condensation would suggest the presence of different pore structures for the different ion exchanged forms. However, this suggestion is contradicted by the reproducibility of the nitrogen isotherms on the identical samples. A more logical explanation would seem to lie in the susceptibility of the argon sorption to changes in the effective saturation vapor pressure within porous media (Harris and Sing, 1967).

Comparison of the specific surface area results for the clay mineral samples saturated with various exchangeable cations using nitrogen and argon gases (columns 2 and 3, Table 1) suggests that the nature of the exchangeable cations has little if any significant effect on the values obtained. For each gas the variation in the specific surface areas obtained for a given clay mineral is within the limits of reproducibility normally acceptable in such measurements.

Nitrogen values are consistently higher on all materials than the corresponding values obtained for argon. Therefore, if nitrogen is taken as the standard adsorbate, larger molecular areas than 14·1 Å^2 are indicated for argon sorption on these materials. It is also evident that the relative molecular areas for nitrogen and

https://doi.org/10.1346/CCMN.1974.0220205 Published online by Cambridge University Press

Table 1. Specific surface areas obtained by application of BET theory and from slope of V–n plots for gas sorption on clay materials

	Surface area ($m^2 g^{-1}$)					
	BET				(V–n)	
Gas	N_2	A	CO_2	Kr	N_2	CO_2
Molecular area $(Å)^2$	16·2	14·1	22·1	19·5	16·2	22·1
Clay						
Sodium A.P.I.–5 Kaolinite	23·1	17·6	12·1	22·2	25·3	20·8
Caesium A.P.I.–5 Kaolinite	22·7	17·6	21·7		24·8	22·8
Calcium A.P.I.–5 Kaolinite	18·9	16·9	13·5		21·6	18·1
Lanthanum A.P.I.–5 Kaolinite	20·7	18·3	12·9		23·5	18·1
Sodium Fithian Illite	95·6	86·8	95·6	123	103	
Caesium Fithian Illite	97·2	87·4	104·4		107	94·6
Calcium Fithian Illite	96·8	89·2	94·3		103	94·9
Lanthanum Fithian Illite	87·2	87·7	86·4		101	92·5
Sodium Willalooka Illite	185		183	200	187	185
Goethite	39·2	35·9	56·3	42·0	43·8	30·4
Hematite	18·0	14·4	25·2	13·8	19·8	16·1
Gibbsite	35·2	29·5	40·9	39·3	42·0	21·7

argon change significantly with the structure of the adsorbent surface.

The most obvious discrepancies occur between the values obtained using CO_2 and those obtained using the other gases under the present assumptions for molecular areas. This is particularly noticeable in the cases of the sodium, calcium and lanthanum saturated kaolinite clays for which the carbon dioxide values are considerably lower than the corresponding nitrogen and argon values. On the other hand, the carbon dioxide areas obtained for the iron and aluminum oxides are considerably higher than the corresponding nitrogen and argon areas. In view of the larger quadrupole moment and high polarizability of the CO_2, greater variation in the area occupied by 1 molecule with variation in the structure of the adsorbent surface would be expected than for the non-polar nitrogen and argon gases. Since the sorbed carbon dioxide could be removed by outgassing overnight at room temp., it is unlikely that chemisorption contributes significantly to the observed effects. The fact that much better agreement is obtained for the three gases on the Fithian illites than for the kaolinites would suggest that the presence of hydroxyl groups on one surface of the plate shaped kaolinite crystals might somehow result in a reduced adsorption of carbon dioxide. This suggestion appears to be contradicted by the considerably higher values obtained for carbon dioxide on gibbsite and goethite. Both materials possess hydroxyl groups on their surfaces. However, a considerably higher specific surface area is also observed with carbon dioxide than with nitrogen for the hematite sample with its oxygen surfaces. This result suggests strongly that an enhanced sorption of the more energetic CO_2 into microporous regions of the oxides, inaccessible to nitrogen and argon, is occurring in a fashion similar to but less dramatic than that observed with carbon dioxide sorption on coal and charcoal materials (Anderson *et al.*, 1965; Walker and Kini, 1965). Explanations for this phenomenon (seemingly anomalous on the basis of molecular size) have been given in terms of activated diffusion of the two gases at their respective adsorption temperature. If this is the case, it is clear that interpretation of the reactivities of these materials based on nitrogen specific surface areas may be subject to some qualification. Just how the presence of hydroxyl groups would reduce so markedly the extent of physical adsorption on kaolinite is not clear.

It is interesting to note from Fig. 4(b) that for both Fithian illite and A.P.I.–5 kaolinite the sorption of CO_2 is apparently significantly dependent on the nature of the exchangeable cation, following the sequence $Cs^+ > Ca^{2+} \approx Na^+ > La^{3+}$ for both materials. Since the isotherms were not obtained in any regular sequence it is unlikely that this order results from some experimental anomaly. The constancy of the differences between the isotherms with increasing relative vapor pressure indicates that they result from initial interactions with the exchangeable ions which displace the remainder of the isotherms with respect to each other.

V–n *plots*

Nitrogen adsorption on a large number of nonporous materials has been shown to produce essentially the same isotherm when plotted in the reduced

https://doi.org/10.1346/CCMN.1974.0220205 Published online by Cambridge University Press

form $n\,(=V/V_m)$ vs p/p_0 (Shull, 1948; Harris and Sing, 1959; Lippens and de Boer, 1965; Pierce, 1968). V–n plots for other materials using this 'universal nitrogen adsorption isotherm' enables deviations from simple monolayer–multilayer adsorption to be detected and the specific surface area of the sample to be calculated from the slop of the plot which yields V_m. In Fig. 5, V–n plots have been constructed for nitrogen adsorption on a number of the materials used in this study using as a standard isotherm the data provided by Shull (1948) for nitrogen adsorption on crystalline materials of large crystal size.

In each case an appreciable range of linearity of the curves is obtained and the specific surface areas obtained from these straight line regions, given in column 6, Table 1, agree well with the corresponding BET values. The linearity of these plots up to the point at which deviations occur indicates that over this region the shape of the isotherms is essentially the same as that obtained on the non-porous reference solids (Shull, 1948). That is, adsorption appears to have taken place entirely by the formation of physically adsorbed layers on the surface with no indication of capillary condensation.

In the case of the illite clays where the pores between the plate-shaped crystals are likely to be slit-shaped,

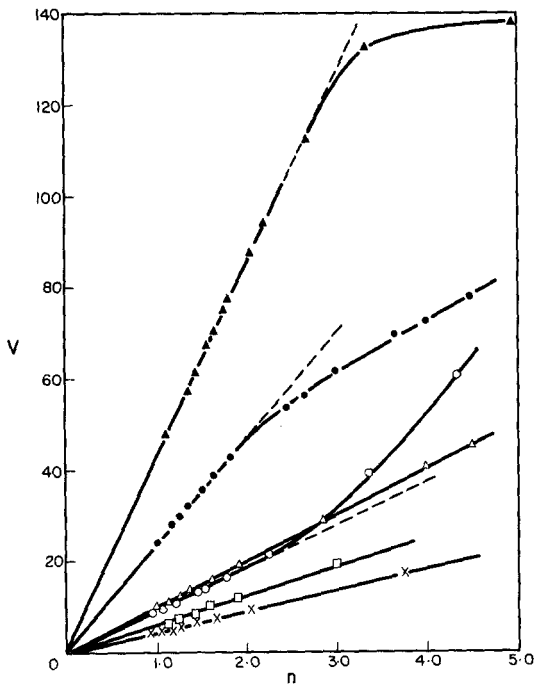

Fig. 5. V–n plots for nitrogen adsorption on ▲ sodium Willalooka illite, ● sodium Fithian illite, □ sodium A.P.I.–5 kaolinite, △ goethite, × hematite, ○ gibbsite.

filling of the pores occurs when the physically adsorbed layers merge in the center of the pore. This filling results in a reduction of the surface area available for subsequent adsorption. For the Fithian illite this point corresponds to the presence of about 2·1 layers on each surface or parallel plate separations of roughly 16 Å (taking the layer thickness as about 4 Å). Similarly for the Willalooka illite, the filling of the smallest pores is completed with approx. 2·4 layers on each surface corresponding to parallel plate separations of some 19 Å. For both materials this filling takes place at relative pressures above about 0·8.

Subsequent desorption would then occur by capillary evaporation governed by the curvature of the semi-cylindrical menisci formed. Both the previous values agree well with the lowest pore sizes indicated by pore size distribution analyses obtained by application of the Kelvin equation, in the form appropriate to semi-cylindrical menisci (Innes, 1957), to nitrogen desorption data on the same materials (Aylmore and Quirk, 1967; Aylmore, unpublished data). These pores are not emptied of capillary condensate until the relative vapor pressure is reduced to about 0·35. Thus, the hysteresis which is almost invariably observed in adsorption–desorption isotherms carried to saturation, results at least partly, for systems such as clay materials containing slit-shaped pores, from a delay in the formation of a meniscus during the adsorption process. These observations are consistent with the 'open-pore' theory of the origin of hysteresis first outlined by Foster (1932). Thus the use of desorption isotherms in pore size distribution analyses on such materials is more valid than the use of adsorption isotherms.

In contrast to the plots for the illite clays, that for gibbsite curves upwards after the initial linear region. This behavior is characteristic of materials in which enhanced sorption, above that corresponding to multilayer formation, occurs as a result of the onset of capillary condensation in transitional pores. The presence of such pores would explain the way in which the argon and nitrogen isotherms in Fig. 3 cross over the corresponding isotherms for goethite at roughly 0·65 relative vapor pressure and thereafter increase more rapidly. The V–n plots for both goethite and hematite remain linear to high n values indicating the absence of transitional pores. Pores in which such condensation occurs are more likely to approximate a cylindrical shape and a relative vapor pressure of 0·65 indicates a pore radius of 30 Å for the onset of condensation.

The apparent susceptibility to change in substrate of the molecular area for CO_2 makes it less feasible to construct a 'universal isotherm' for this gas. However,

https://doi.org/10.1346/CCMN.1974.0220205 Published online by Cambridge University Press

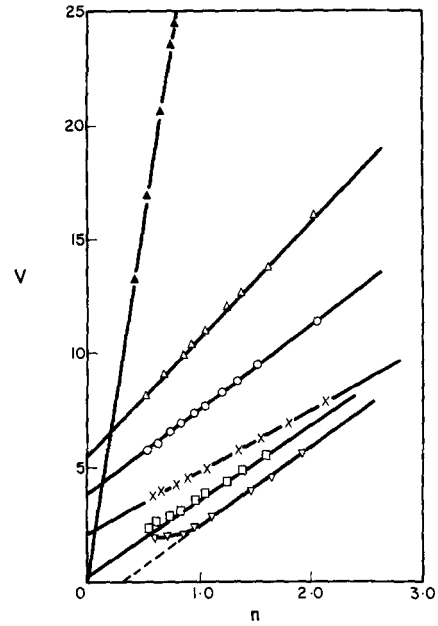

Fig. 6. V–n plots for carbon dioxide adsorption on △ goethite, × hematite, ○ gibbsite, ▽ sodium A.P.I.–5 kaolinite, □ caesium A.P.I.–5 kaolinite, ▲ sodium Willalooka illite.

an interesting comparison can be made between the various materials using the carbon dioxide isotherm on sodium Fithian illite as a standard. This isotherm was chosen because the carbon dioxide area agrees well with the nitrogen area under the present assumptions. In addition, the adsorption of carbon dioxide on Fithian illite is completely reversible up to high relative vapor pressures indicating the absence of capillary condensation. The V–n plot obtained in this way for carbon dioxide sorption on sodium Willalooka illite, shown in Fig. 6, yields a straight line passing through the origin. The specific surface area obtained from the slope agrees well with both the nitrogen and carbon dioxide BET values (Table 1). In contrast, similar V–n plots for carbon dioxide sorption on goethite, hematite and gibbsite provide good straight lines with positive intercepts on the volume axis. This behavior is characteristic of materials in which micropore filling has occurred and strongly supports the previous interpretation of the larger BET specific surface areas obtained with carbon dioxide than with nitrogen. A simple variation in molecular area with respect to that on the illite would alter the slope of the V–n plot for these materials but the plots would still pass through the origin. The specific surface areas obtained from the slopes of these lines (column 7, Table 1) are smaller than the nitrogen BET areas; however, this difference could be accounted for either by variations in molecular area or degree of accessibility to nitrogen and carbon dioxide sorption in the different materials.

The V–n plot for carbon dioxide sorption on sodium A.P.I.–5 kaolinite is equally interesting. The linear region of the plot gives a specific surface area close to that for the BET nitrogen value but intersects the abscissa. Below $n \approx 0{\cdot}9$ there is little change in sorption at least down to an n value of about 0·6. This suggests that the initial sorption of carbon dioxide on this material takes places with a considerably larger effective cross-sectional area per molecule, presumably as a result of some specific interaction, than occurs with the illite–clay. With the completion of this layer a change in state for subsequent adsorption occurs allowing normal multilayer formation to proceed. Although not shown in Fig. 6, similar effects occur with both the calcium and lanthanum saturated kaolinites. However in the case of the cesium saturated kaolinite this effect is less evident and a more normal V–n plot is obtained (Fig. 6), providing a specific surface area in excellent agreement with both the nitrogen and carbon dioxide BET values. The structure breaking properties of the large cesium ion thus appear to hinder the formation of a specifically adsorbed layer.

It is possible that the development of this dilute layer arises from an interaction between the large permanent quadrupole moment of the carbon dioxide molecule and the electric field gradient in the neighborhood of the exchangeable cations. Thus, the strength of the interaction would increase with increasing ionic charge and decrease with increasing ionic dia. Alternatively, it seems more likely that the development of a surface induced structure in the first layer of adsorbed molecules is disrupted to an extent determined by the size and frequency of cations on the surface. Although the initial adsorption of carbon dioxide on both illite and kaolinite is subject to the nature of the exchangeable cation, the sorption on kaolinite is clearly much more inhibited, despite similar surface densities of charge for both materials. This behavior is at present under more detailed study.

CONCLUSIONS

It is clear that specific surface areas obtained by application of the BET theory to gas sorption isotherms on clay mineral systems are subject to significant variations in apparent molecular areas with variations in surface structure, exchangeable cation and microporosity. Argon sorption appears the least subject to such variations at lower relative vapor pressure and is thus likely to provide the most reproducible areas by application of the BET theory. Uncertainties in the effective saturation vapor pressure for argon sorption at

https://doi.org/10.1346/CCMN.1974.0220205 Published online by Cambridge University Press

higher relative vapor pressures where capillary condensation occurs, and the reproducibility of the nitrogen isotherms in this region, indicate that nitrogen is a better choice for pore size distribution analyses based on the Kelvin equation.

The range of linearity of the V–n plots for nitrogen sorption on the clay minerals indicates that adsorption in the slit-shaped pores within these systems takes place largely by the formation of physically adsorbed multilayers on the surfaces. With the filling of the pores desorption would then be governed by the curvature of the semi-cylindrical meniscii formed. Hysteresis in such systems thus results at least partly from a delay in the formation of a meniscus during the adsorption process in accord with the 'open-pore' theory.

The larger specific surface areas obtained by application of the BET theory and the positive intercepts on the volume axis in the V–n plots for carbon dioxide sorption at 196°K on goethite, hematite and gibbsite suggest the presence of micropores in these oxides, inaccessible to nitrogen, argon and krypton sorption at 78°K. Interpretations of the reactivities of these materials based on nitrogen, argon or krypton sorption would not take such micropores into account. Thus for many purposes, particularly in comparisons between similar oxides, the greater penetration and absence of capillary condensation indicated by the V–n plots for carbon dioxide sorption at 196°K, may make this gas a more appropriate adsorbate than the conventional use of nitrogen and argon.

The lower BET specific surface areas and the shape of V–n plots for carbon dioxide sorption on sodium, calcium and lanthanum saturated kaolinite suggest that an initial specific adsorption of carbon dioxide on these kaolinites is followed by a change in state for subsequent adsorption allowing normal multilayer formation to proceed.

Acknowledgements—This paper results from a project financed by the Australian Research Grants Committee whose support is gratefully acknowledged.

REFERENCES

Anderson, R. B., Bayer, J. and Hofer, L. J. E. (1965) Determining surface areas from CO_2 isotherms: *Fuel* **44,** 443–452.

Aristov, B. C. and Kiselev, A. V. (1963) Effect of dehydration of silica surface on the adsorption isotherms for gaseous nitrogen and argon: *Russian J. Phys. Chem.* **37,** 1359–1363.

Aylmore, L. A. G. and Quirk, J. P. (1967) The micropore size distributions of clay mineral systems: *J. Soil Sci.* **18,** 1–17.

Aylmore, L. A. G., Sills, I. D. and Quirk, J. P. (1970) Surface area of homoionic illite and montmorillonite clay minerals as measured by the sorption of nitrogen and carbon dioxide: *Clays and Clay Minerals* **18,** 91–96.

Beebe, R. A., Beckwith, John B. and Honig, Jurgen M. (1945) The determination of small surface areas by krypton adsorption at low temperatures: *J. Am. Chem. Soc.* **67,** 1554–1558.

Brunauer, S., Emmett, P. H. and Teller, E. (1938) Adsorption of gases in multimolecular layers: *J. Am. Chem. Soc.* **60,** 309–310.

Carruthers, J. D., Payne, D. A., Sing, K. S. W. and Stryker, L. J. (1971) Specific and non-specific interactions in the adsorption of argon, nitrogen and water vapour on oxides: *J. Colloid Interface Sci.* **36,** 205–216.

Emmett, P. H. and Brunauer, S. (1937) The use of low temperature van der Vaals adsorption isotherms in determining the surface area of iron synthetic ammonia catalysts: *J. Am. Chem. Soc.* **59,** 1553–1564.

Foster, A. G. (1932) The sorption of condensible vapours by porous solids—I. The applicability of the capillary theory: *Trans. Farad. Soc.* **28,** 645–657.

Gregg, S. J. and Sing, K. S. W. (1967) *Adsorption, Surface Area and Porosity*. Academic Press, New York.

Harkins, W. D. and Jura, G. (1944) Surface of solids X, XII and XIII: *J. Am. Chem. Soc.* **66,** 919–927.

Harris, M. R. and Sing, K. S. W. (1967) Use of argon adsorption for the determination of specific surface area: *Chem. Ind.* 757–758.

Innes, W. B. (1957) Use of a parallel plate model in calculation of pore size distribution: *Anal. Chem.* **29,** 1069–1073.

Joyner, L. G. (1958) *Scientific and Industrial Glass Blowing and Laboratory Techniques* (Edited by Barr, W. E. and Anhorn, V. J.), Chap. 12. Instruments Publishing Co., Pittsburgh.

Lippens, B. C. and de Boer, J. H. (1965) Studies on pore systems in catalysis—V. The t method: *J. Catalysis* **4,** 319–323.

Pierce, Conway (1968) The universal nitrogen isotherm: *J. Phys. Chem.* **72,** 3673–3676.

Pierce, Conway and Ewing, Bland (1964) Areas of uniform graphite surfaces: *J. Phys. Chem.* **68,** 2562–2568.

Shull, C. G. (1948) The determination of pore size distribution from gas adsorption data: *J. Am. Chem. Soc.* **70,** 1405–1414.

Sing, K. S. W. (1968) Empirical method for analysis of adsorption isotherms: *Chem. Ind.* 1520–1521.

Résumé—Les isothermes de sorption de quatre gaz (N_2, A, Kr et CO_2) utilisés couramment pour les mesures de surface spécifique et de structure des pores, ont été déterminées avec précision sur un certain nombre de minéraux argileux et d'oxydes.

Les surfaces spécifiques obtenues en appliquant la théorie de BET à ces isothermes montrent bien jusqu'à quel point les surfaces projetées apparentes de ces gaz sorbés varient avec la structure superficielle, le cation échangeable et la microporosité.

Les courbes V–n pour l'adsorption d'azote sur les matériaux étudiés, en considérant l'adsorption d'azote sur des matériaux cristallins de grande taille particulaire comme une isotherme de référence, ont des

domaines de linéarité appréciables dans chaque cas. Les surfaces spécifiques obtenues à partir de ces droites sont en accord avec les valeurs BET correspondantes. La linéarité de ces diagrammes pour les illites indique qu'il n'y a pas de condensation capillaire et que l'adsorption dans les pores en forme de fente se fait, pour une grande part, par suite de la formation de couches adsorbées physiquement sur les surfaces.

Des surfaces spécifiques BET beaucoup plus grandes qu'avec la sorption à 78°K de l'azote, de l'argon et du krypton, ont été obtenues avec la sorption du gaz carbonique à 196°K sur la goethite, l'hématite et la gibbsite. On fait l'hypothèse que la sorption accrue du CO_2 dans la microporosité des oxydes inaccessible aux autres gaz, relève d'un processus similaire à celui que l'on observe fréquemment sur les carbones et charbons de bois. Les courbes V–n pour la sorption du CO_2 sur ces matériaux étayent cette conclusion si l'on utilise l'illite comme isotherme de référence.

Sur la kaolinite, la sorption du gaz carbonique conduit à des surfaces spécifiques BET considérablement plus basses que celles que l'on obtient avec la sorption de l'azote, de l'argon et du krypton. La forme des courbes V–n pour la sorption du CO_2 sur la kaolinite comparée à l'illite suggère qu'une adsorption spécifique initiale du CO_2 sur la kaolinite est suivie par un changement d'état de cette couche adsorbée lorsqu'elle est complète, ce qui permet par la suite la formation d'un système normal à plusieurs couches adsorbées.

Kurzreferat—Sorptionsisothermen für 4 Gase (N_2, A, Kr, CO_2), die gewöhnlich für Messungen der spezifischen Oberfläche und der Porenstruktur benutzt werden, wurden für eine Anzahl von Tonmineralen und Oxidsystemen genau bestimmt. Die spezifischen Oberflächen, die durch Anwendung der BET-Theorie auf diese Isothermen erhalten wurden, illustrieren das Ausmaß, in dem die scheinbaren Querschnittsflächen für diese Gase mit der Oberflächenstruktur, dem austauschbaren Kation und der Feinporosität schwanken.

V-n-Diagramme für die Stickstoffadsorption an diesen Stoffen unter Verwendung der Stickstoffadsorption an grobkristallinem Material als Standardisotherme liefern in jedem Fall merkliche Linearitätsbereiche. Die spezifischen Oberflächen, die von diesen linearen Bereichen der Diagramme erhalten wurden, stimmen gut mit den zugehörigen BET-Werten überein. Die Linearität dieser Kurven für Illittone zeigt, daß Kapillarkondensation fehlt und daß die Absorption in spaltförmigen Poren weitgehend durch Bildung physikalisch adsorbierter Schichten an den Oberflächen stattfindet. Viel größere spezifische BET-Oberflächen wurden aus der Kohlendioxidsorption bei 196°K an Goethit, Hämatit und Gibbsit erhalten als aus der Sorption von Stickstoff, Argon und Krypton bei 78°K. Es wird angenommen, daß die verstärkte Sorption von CO_2 in die Mikroporenbereiche der Oxide, die für andere Gase unzugänglich sind, in ähnlicher Weise erfolgt, wie es häufig für Kohle und Holzkohle beobachtet wurde. V-n-Kurven für die CO_2-Sorption an diesen Stoffen unter Verwendung der für Illitton erhaltenen als einer Standardisotherme stützen diese Schlußfolgerung. Bedeutend geringere spezifische BET-Oberflächen wurden aus der CO_2-Sorption an Kaolinit erhalten als aus der Sorption von Stickstoff, Argon und Krypton. Die Form der V-n-Kurven für die CO_2-Sorption an Kaolinit im Vergleich zu Illit legt nahe, daß einer anfangs spezifischen CO_2-Sorption an Kaolinit eine Zustandsänderung mit der Vervollständigung dieser Schicht folgt, die es gestattet, daß die Bildung einer normalen Vielschicht abläuft.

Резюме — Изотермы сорбции четырех газов (N_2, A, Kr и CO_2), обычно используемых для измерения специфических площадей поверхности и структуры пор, точно определяли на ряде глинистых минералов и систем окислов. Специфические площади поверхности, полученные применением теории B.E.T. к этим изотермам, иллюстрируют до какой степени очевидные профили этих сорбированных газов меняются в зависимости от структуры поверхности, катионообмена и микропористости.

Для определения адсорбции азота на этих материалах построили V–n-диаграмму, используя адсорбцию азота на крупнокристаллических материалах в качестве стандартной изотермы и получили заметные области линейного изменения в каждом случае. Специфические площади поверхности, полученные посредством этих графиков прямых линий почти полностью соответствуют значениям B.E.T. Линейность этих графиков для иллитовой глины, указывает на отсутствие капиллярной конденсации и на адсорбцию в щелеобразных порах, происходящей большей частью вследствие образования на поверхности физически адсорбированных слоев.

Более крупные специфические площади поверхности B.E.T. были получены сорбцией угольного ангидрида при температуре 196°K на гетите, гематите и гибсите, чем от сорбции азота, аргона и криптона при температуре 78°K. Предполагают, что улучшенная сорбция CO_2 в микропоры окислов, недоступные для других газов, происходит таким же образом, как это нередко наблюдается с углем и древесным углем. V–n-диаграмма сорбции CO_2 на этих материалах, подтверждает этой заключение.

При сорбции CO_2 на каолине получили значительно меньшие специфические площади поверхности B.E.T., чем при сорбции азота, аргона и криптона. Форма V–n-диаграммы сорбции CO_2 на каолине по сравнению с иллитом наводит на мысль, что за начальной удельной сорбцией CO_2 на каолине следует изменение состояния слоя, допуская продолжение нормального образования свиты пластов.

https://doi.org/10.1346/CCMN.1974.0220205 Published online by Cambridge University Press